

# In Teacher We Trust: Deep Network Compression for Pedestrian Detection

Jonathan Shen<sup>1</sup>  
Carnegie Mellon University  
jshen2@andrew.cmu.edu

Noranart Vesdapunt<sup>1</sup>  
Carnegie Mellon University  
nvesdapu@andrew.cmu.edu

Vishnu N. Boddeti  
Michigan State University  
vishnu@msu.edu

Kris M. Kitani  
Carnegie Mellon University  
kkitani@cs.cmu.edu

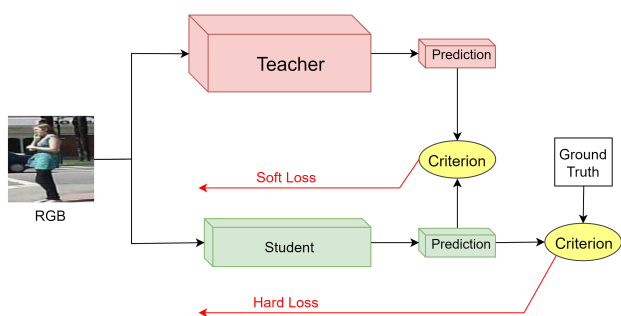
## Abstract

Deep convolutional neural networks continue to advance the state-of-the-art in many domains as they grow bigger and more complex. It has been observed that many of the parameters of a large network are redundant, allowing for the possibility of learning a smaller network that mimics the outputs of the large network through a process called Knowledge Distillation. We show, however, that standard Knowledge Distillation is not effective for learning small models for the task of pedestrian detection. To improve this process, we introduce a higher-dimensional hint layer to increase information flow. We also estimate the uncertainty in the outputs of the large network and propose a loss function to incorporate this uncertainty. Finally, we attempt to boost the complexity of the small network without increasing its size by using as input hand-designed features that have been demonstrated to be effective for pedestrian detection. For only a 2.8% increase in miss rate, we have succeeded in training a student network that is 8 times faster and 21 times smaller than the teacher network.

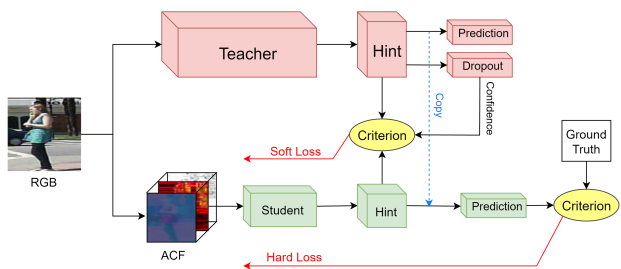
## 1. Introduction

State-of-the-art deep convolutional neural networks are extremely large and require a vast amount of resources both to train and test. For example, the classic VGG-16 image classification network [27] contains 138 million parameters, and the more recent ResNet-200 [15] still contains over 60 million parameters. In the realm of pedestrian detection, the top three approaches as measured on the Caltech Pedestrian Dataset [10] consist of MSCNN [3], RPN+BF [29], both built upon the Faster-RCNN [24] architecture containing over 100 million parameters, and SA-FastRCNN [20] which features a network with over 30 million parameters.

<sup>1</sup>Contributed equally.



(a) Standard: student network learns from teacher guidance (soft loss) and ground truth (hard loss).



(b) Ours: student network uses ACF features as input and learns from teacher's hint layer outputs and covariances.

Figure 1: Comparison between standard Knowledge Distillation (a) and our pipeline (b).

The larger a network is, the more disk space, memory, and energy it consumes while being slower to evaluate.

We are interested in the possibility of designing small pedestrian detection models that can be stored and used on a mobile computing platform with limited resources, *e.g.*, Nvidia TX1 that has 4GB of memory. However, we would like to maintain a similar level of performance as the larger and more powerful deep network. Fortunately, recent work has shown that many of the large deep networks contain many redundant parameters [19, 7]. In theory, the models

could be much smaller.

In this work, we adopt the process of Knowledge Distillation (KD) [17] to train a small *student* network to mimic the large *teacher* network. KD was developed for tasks like classification on the ImageNet dataset [26]. The key idea is that the soft activations of the output layer of a teacher network is a richer signal for learning a network compared to using the indicator vector typically used as a ground truth label (*e.g.*, one for the true category and zero elsewhere). The intuition is that the soft output distribution of a well-trained network encodes extra information about the high-level correlation between categorical outputs.

While this idea translates to classification tasks with many categories, the amount of information revealed through the output layer for a low-dimensional classification task is less informative. Specifically in the case of pedestrian classification, the output space is binary and the soft distribution is not sufficiently informative. To retain the ability to learn from correlations between high-level features, we propose to distill the knowledge in the layer just before the output layer (*e.g.*, typically a fully connected layer with high dimensionality) and use it as the hint layer for guiding the student network learning process.

When the output of a teacher network is used to train a student network using a large dataset of unlabeled data, there is no guarantee that the output of the teacher network is error free. In this scenario, the policy behind KD is to train the student to mimic the teacher’s response regardless of potential mistakes. While this process will indeed enable the student to faithfully mimic the performance of the teacher network, it will also be prone to making the same mistakes as the teacher. Therefore, blindly mimicking the teacher’s knowledge, both correct and incorrect, may not be the optimal learning process for the student.

Intuitively, if the teacher could convey some notion of confidence about its output, then the student could use that side information to trust the teacher’s knowledge more or less during the learning process. Paying more attention to the knowledge that the teacher is more confident about enables the student to allocate their limited learning capacity towards more accurately distilling the teacher’s knowledge. To produce a measure of teacher confidence, we follow the insights in [11] and utilize dropout at test time to get uncertainty estimates of the teacher outputs. We fit a Gaussian distribution to the teacher outputs that is then used during the teacher-student training process. Specifically, we propose a modified loss function that incorporates uncertainty information for training.

As models are compressed to be smaller at extreme rates, we hypothesize that the lower layers of the small deep networks will have a harder time learning useful features for pedestrian detection. Historically, we have observed that carefully designed image features specific to the task of

pedestrian detection can have a meaningful impact on performance. Interestingly, recent work using end-to-end deep networks have shown that features learned with a deep network are better than traditional pedestrian detection features [18]. One theory is that very deep convolutional neural networks are able to learn features that are more powerful than hand-designed features. If this is indeed the case, we hypothesize that very small networks may not have the capacity to do so, and traditional feature extraction may help improve the performance of small deep networks. We investigate this hypothesis using Aggregate Channel Features (ACF) [8] which have been proven to be effective features for pedestrian detection.

**Contributions.** In this paper we propose to use Knowledge Distillation to compress a large network for pedestrian classification. We explore variations on the training process by (1) learning from the outputs of a high-level hint layer before the final fully-connected layer to compensate for the lack of sufficient information in that layer for knowledge distillation, (2) introducing a loss function that takes into account the confidence of the teacher network, and (3) evaluating the role of classical pedestrian specific features like Aggregate Channel Features as input to small student networks.

## 2. Related Work

**Network Pruning** The earliest studies into network size reduction came in the form of weight pruning, motivated by the need for regularization. These methods use the magnitude of the weights [13] or the Hessian of the loss function [19, 14] to prune away less useful weights. Apart from pruning weights, Srinivas and Babu [28] devised a method for pruning neurons directly without the use of any training data. These pruning approaches remove a significant amount of the uninformative parts of the network and results in lower computation costs and storage requirements. Although the number of parameters are reduced through pruning, the basic structure (*e.g.*, number of layers) of the network remains unchanged.

**Parameter Sharing** Han *et al.* [12] introduced a multi-step pipeline with pruning, weight clustering and Huffman encoding. An orthogonal approach uses hashing or bucketing to quantize various parts of the model [4, 21]. Cheng *et al.* [5] enforce a circulant matrix model on the fully-connected layers to exploit faster computation and smaller model size via Fast Fourier Transforms. By quantizing and sharing parameters, the amount of space needed to store the network representation is reduced.

**Matrix Decomposition** Neural network weights can be treated as matrices and compressed through matrix decomposition. Denil *et al.* [7] use a low rank decomposition of the weight matrices together with a sparse dictionary

learned from an autoencoder to reduce the number of parameters. Novikov *et al.* [22] apply the Tensor-Train decomposition [23] to compress the weight matrices in the fully-connected layers.

**Transfer Learning.** While the above methods compress an existing network directly, the underlying architecture remains bulky with the same width and depth as before. An alternative is to consider transferring the knowledge to a new smaller network. This produces a much more compact model with dense weights instead of sparse weights. Moreover, it is possible to then apply the above methods on top of the new network to reduce it further.

Ba and Caruana [1] showed that it is possible to train a shallower but wider student network to mimic a teacher network, performing almost as well as the teacher. Hinton *et al.* [17] generalized this idea by training the student to learn from both the teacher and from the training data, naming this process Knowledge Distillation (KD). They demonstrated that students trained this way outperform those trained directly using only the training data.

FitNets [25] use Knowledge Distillation with many intermediate hint layers to train a thinner but deeper student network containing fewer parameters that outperforms even the teacher network. The design of such networks relies on the ability of the network designer to find an appropriate layer-wise strategy to match the intermediate layers of the teacher network to corresponding intermediate layers in the student network. Although FitNets require heavy human intervention to generalize to a new teacher/student network, the approach is very effective since the student network can be trained in a step-wise manner using many supervisory signals.

### 3. Knowledge Distillation

The process of Knowledge Distillation (KD) for classification networks is to train the student from the predictions of the teacher network in addition to the ground truth *hard targets* (Figure 1a). However, with a standard soft maximum (softmax) classification layer, the teacher predictions will often be very similar to the hard targets with one class having probability close to 1 and the other classes having probabilities close to 0. So, instead, a variant of the softmax function which includes a temperature parameter  $T$  is used instead to produce *soft targets*,

$$\text{softmax}(\mathbf{L}, T) = \frac{\exp(\mathbf{L}/T)}{\sum_j \exp(L_j/T)}. \quad (1)$$

When  $T = 1$ , this is the standard softmax function, while higher values of  $T$  produce a smoother probability distribution over the classes.  $\mathbf{L}$  are the input logits to the softmax layer, and are also the outputs of the fully-connected layer before it.

The loss function  $\mathcal{L}$  used for training the student is a combination of the soft loss  $\mathcal{L}_{\text{soft}}$ , the cross-entropy loss between the soft outputs of the student and teacher, as well as the hard loss  $\mathcal{L}_{\text{hard}}$ , the standard classification cross-entropy loss between the student outputs and the ground truth labels:

$$\mathcal{L}_{\text{soft}} = \mathcal{H}(\text{softmax}(\mathbf{L}_S, T), \text{softmax}(\mathbf{L}_T, T)) \quad (2)$$

$$\mathcal{L}_{\text{hard}} = \mathcal{H}(\mathbf{Y}_S, \mathbf{Y}_{\text{GT}}) = \mathcal{H}(\text{softmax}(\mathbf{L}_S, 1), \mathbf{Y}_{\text{GT}}) \quad (3)$$

$$\mathcal{L} = \mathcal{L}_{\text{soft}} + \lambda \mathcal{L}_{\text{hard}}. \quad (4)$$

## 4. Proposed Approach

A graphical outline of our augmented KD pipeline can be found in Figure 1b. Here we explain the various parts of the pipeline and the motivations behind them.

### 4.1. Single High-level Hint Layer

KD was developed for ImageNet classification with the idea that the 1000-dimensional prediction from the teacher is much more informative than the single ground truth label. But for pedestrian classification where there are only 2 outputs (pedestrian / no pedestrian), this difference between hard and soft outputs is much less pronounced. Since the output of a softmax function sums up to 1 for every value of temperature  $T$ , the degree of freedom of binary soft targets is actually only 1-dimension.

To increase the dimensionality of the data that the student learns from, we use a hint layer, a fully-connected (FC) layer just before the final FC layer, and train the student to match the outputs of the hint layer instead. If the student network can perfectly match the hint layer outputs, we can simply copy over the teacher’s final FC layer and the student will be able to mimic the teacher’s outputs. Even if the student cannot perfectly match the hint layer outputs, the weights from the teacher’s final FC layer still serve as a good initialization for the student’s final FC layer, which will be fine-tuned through the hard loss coming from the ground truth labels.

This idea of matching hint layers at intermediate layers has been explored in FitNets [25]. As the primary goal of FitNets is to learn a very deep (yet thin) network as the student model, an entire sequence of hint layers in the teacher network are used to sequentially train a sequence of intermediate ‘guided’ layers of the student network. The selection of hint layers and the selection of guided layers, as well as the sequential pairings between hint/guide must be designed by the network designer. Furthermore, to account for the potential difference in dimensionality and receptive field between hint/guide pairings, an additional convolutional regression layer must be added during training. Compounding the design burden further, the network designer must also decide on the parameters and structure of the primitive module used by the student network. In contrast to FitNets,

our proposed method requires significantly less engineering. As a consequence, our method is more generalizable, as it only requires one pairing between a high-level (late in the network) hint layer and the output of our student network.

As an aside, care must be taken when the activation for the hint layer is a rectified linear (ReLU) nonlinearity, in which case it is advised to match the values before passing them through the ReLU function. This is because the ReLU function discards information of negative values, and also because the gradient from where the student predicts a negative value is ignored, leading to instabilities in training.

## 4.2. Learning With Confidence

There will be cases where the teacher makes mistakes and predicts differently from the ground truth. The policy behind KD is to train the student to mimic the teacher regardless of the mistakes, relying on the hard losses to nudge the outputs towards the correct label. This results in a tension between the soft and hard losses, each producing a gradient for the opposite label.

This tension can be relaxed if the teacher has an estimate of prediction confidence. Intuitively, if the teacher reports that it is very confident about its prediction, then the student should trust the teacher more, and if the teacher instead reports that it is not confident about its prediction, then the student should balance mimicking the teacher with predicting the correct label. The underlying assumption is that the teacher is more likely to be confident about examples that they predict correctly. There will be cases where the teacher is very confident yet mistaken, but we believe that it is important for the student not to disregard the teacher in these cases.

In [11], the authors draw a theoretical link casting dropout as a Bayesian approximation of Gaussian Processes. Following their ideas, we enable dropout during test time and forward the same input through the model  $N$  times. Each pass can be thought of as the output of a single model sampled from an ensemble. From this, the sample mean  $\bar{\mathbf{Y}}$  and covariance  $\hat{\Sigma}$  of the outputs of the ensemble can be estimated.

By doing so, we are fitting a multivariate Gaussian distribution to the teacher outputs, from which it is possible to measure the likelihood of the student output as being drawn from the distribution. In particular, the likelihood of the student output is:

$$p(\mathbf{Y}_S) = \frac{\exp\left(-\frac{1}{2}(\mathbf{Y}_S - \bar{\mathbf{Y}}_T)^T \hat{\Sigma}^{-1}(\mathbf{Y}_S - \bar{\mathbf{Y}}_T)\right)}{\sqrt{(2\pi)^k |\hat{\Sigma}|}}. \quad (5)$$

Maximizing the log-likelihood of Equation 5 is equiva-

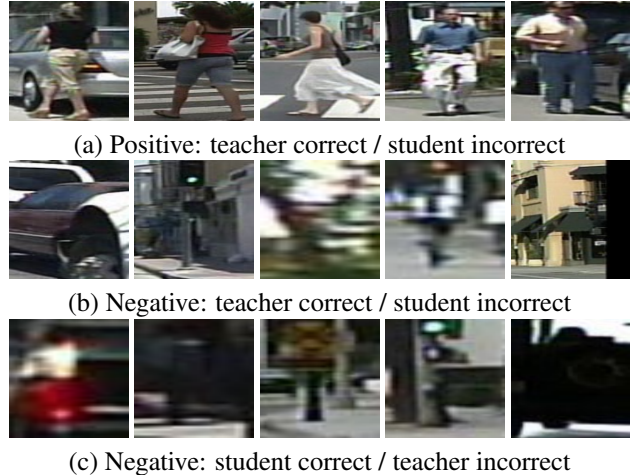


Figure 2: Example of disagreements between teacher (ResNet-200) and student (ResNet-18-Small-*RGB-Hint-Conf*).

lent to minimizing the following loss function:

$$\mathcal{L}_{\text{soft}} = (\mathbf{Y}_S - \bar{\mathbf{Y}}_T)^T \hat{\Sigma}^{-1} (\mathbf{Y}_S - \bar{\mathbf{Y}}_T). \quad (6)$$

This function is the square of the Mahalanobis distance. Compared to the mean-square distance, it is smaller along dimensions of high variability, consistent with our idea of reporting smaller gradients for teacher outputs with low confidence.

The dimensionality of the covariance matrix can be very large when applied to layers with many parameters. Since the loss function requires the inversion of covariance matrix, the number of samples  $N$  must be larger than the dimensionality of the teacher's output. To speed this process up, the output from the time consuming convolutional layers can be cached, and only the last few layers with dropout need multiple passes, so the additional overhead during training is low. The aim of this new loss is to reduce the number of disagreements between the teacher and student (examples in Figure 2).

## 4.3. Hand-designed Features as Input

Before deep learning became mainstream, computer vision was dominated by the use of task-specific features discovered through extensive experimentation. For example, the advent of HOG features [6] was ground-breaking in the development of pedestrian detection, and the introduction of Integral Channel Features [9] brought about another revolution, leading to the discovery of many derivative features such as Aggregate Channel Features [8] and Checkerboards features [30], the latter of which is competitive with state-of-the-art.

These hand-designed features are largely ignored in deep learning to heed the way for end-to-end learning. In fact,

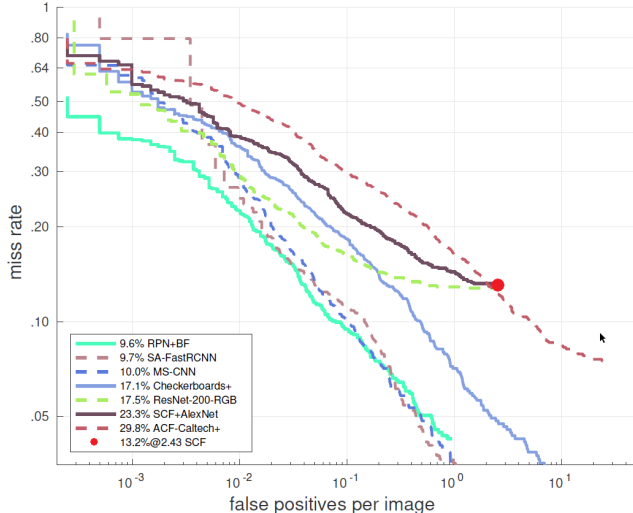


Figure 3: Our ResNet-200 teacher network ranks among the top pedestrian detection methods and is used to analyze our KD approach.

in [18], it was observed that there was no improvement in neural networks trained using hand-designed features compared to those trained using raw RGB images as input. However, the model was very large, so it is possible that this added capacity enabled the network to learn features that outperform the hand-designed features. The same may not be true for a small model, in which case it may be reasonable to expect that by using these hand-designed features as input, a smaller model could be improved. The use of hand-designed features as input can also be thought of as attaching a fixed layer to the front of the network, pre-trained through years of human research.

For this reason, we explore training our student networks using Aggregate Channel Features (ACF) as input. We choose ACF because it offers a good trade-off between detection accuracy and speed, taking less than 10ms to compute for a  $640 \times 480$  image on a single CPU [8]. ACF consist of 10 channels: the LUV color channels, gradient magnitude, and six oriented gradient bins. The input image is first converted into these 10 channels, then, within each channel, pixels are divided into  $4 \times 4$  blocks and summed. Note that when we train the student using ACF features as input, the input to the teacher remains the original RGB image. Whether the student is trained on RGB or ACF, they learn from the exact same teacher.

## 5. Experimental Setup

We perform all training and evaluation on the Caltech Pedestrian Dataset [10]. Following standard practice, we use the first 5 sequences as the training set, the 6th sequence as the validation set, and the last 5 sequences as

	ResNet-200	ResNet-18
conv1	$7 \times 7 \times 64$ , stride 2 $3 \times 3$ pool, stride 2	$7 \times 7 \times 64$ , stride 2 $3 \times 3$ pool, stride 2
conv2_x	$\begin{bmatrix} 3 \times 3 \times 64 \\ 3 \times 3 \times 64 \\ 3 \times 3 \times 256 \end{bmatrix}$ x3	$\begin{bmatrix} 3 \times 3 \times 64 \\ 3 \times 3 \times 64 \end{bmatrix}$ x2
conv3_x	$\begin{bmatrix} 3 \times 3 \times 128 \\ 3 \times 3 \times 128 \\ 3 \times 3 \times 512 \end{bmatrix}$ x24	$\begin{bmatrix} 3 \times 3 \times 128 \\ 3 \times 3 \times 128 \end{bmatrix}$ x2
conv4_x	$\begin{bmatrix} 3 \times 3 \times 256 \\ 3 \times 3 \times 256 \\ 3 \times 3 \times 1024 \end{bmatrix}$ x36	$\begin{bmatrix} 3 \times 3 \times 256 \\ 3 \times 3 \times 256 \end{bmatrix}$ x2
conv5_x	$\begin{bmatrix} 3 \times 3 \times 512 \\ 3 \times 3 \times 512 \\ 3 \times 3 \times 2048 \end{bmatrix}$ x3	$\begin{bmatrix} 3 \times 3 \times 512 \\ 3 \times 3 \times 512 \end{bmatrix}$ x2
classifier	avgpool dropout FC(2048, 64, ReLU) FC(64, 2, softmax)	avgpool FC(512, 64, ReLU) FC(64, 2, softmax)

Table 1: Architectural details for the base ResNet models for experiments.

the test set. We follow the setup of Caltech10x in [18] and sample every 3rd frame for training. We use the ‘Reasonable’ configuration when testing on the Caltech test set, which samples every 30th frame and includes only pedestrians without significant occlusion with a minimum height of 50 pixels and the labels “people” and “person?” are excluded. Evaluation is performed using the official evaluation script, which computes a curve of the logarithm of the number of false positives per image versus the miss rate. A value for the log-average miss rate is also calculated, and a lower value indicates a better result. Our training set uses ground truth patches as well as patches with Intersection-over-Union (IoU) greater than 0.5 as positive patches, and patches with IoU less than 0.5 as negative patches. There are 31, 129 positive patches and 748, 139 negative patches in the training set.

### 5.1. Teacher and Student Models

For all of our teacher-student pairs, we use ResNet as the primitive module to ensure that the change in performance is due to our proposed KD process and not the difference between primitive convolutional modules (*e.g.*, Inception versus ResNet).

**Teacher Network** For our teacher network, we use pre-activation ResNet-200 [16] pre-trained on ImageNet, augmented with dropout and a 64-dimensional hint layer, then fine-tuned on our training set. Architectural details of the teacher network are give in Table 1. In Figure 3 we also show the state of the art performance on the Caltech pedestrian dataset to show the relative performance of our teacher network ResNet-200. Although, ResNet-200

Model	#Parameters	Compression
ResNet-200	63M	1×
ResNet-18	11M	6×
ResNet-18-Thin	2.8M	22×
ResNet-18-Small	157K	400×
AlexNet	57M	1×

Table 2: Comparison of the sizes of our various models and AlexNet.

is not the absolute best performing model (leader board is constantly changing), it performs comparably and we believe that it is a reasonable teacher network. We would like to emphasize here that the focus of this work is on the ability to distill knowledge to an extremely small network and not necessarily to beat the state-of-the-art. Using ResNet allows us to analyze the impact of knowledge distillation while avoiding the complexities of accounting for differences in architectural strategy.

**Student Network** We use pre-activation ResNet-18 [16] pre-trained on ImageNet augmented with a 64-dimensional hint layer as the basis for our student networks. We experiment with three versions: (1) unmodified ResNet-18, (2) ResNet-18-Thin which cuts the number of channels for every layer in half, and (3) ResNet-18-Small which fixes every layer at 32 channels. A detailed overview of ResNet-18 is given in 1. Both teacher and student model architectures use  $224 \times 224$  input patches. Pool refers to a max-pooling layer, FC refers to a fully-connected layer, and avgpool refers to a global average pooling layer. All convolutional layers include batch normalization and ReLU activation. The first convolution layer for conv{3,4,5} have a stride of 2.

Student model compression rates are given in Table 2. Notice the extreme compression rate of ResNet-18-Small at 400× when compared to AlexNet or ResNet-200. For our student network using pedestrian specific input features, we follow [18] and use the publicly available SquaresChnFtrs [2] region proposals. Using the same region proposal as [18] also gives us a fair comparison between AlexNet and our student network. The oracle miss rate of this region proposal is 13.2% at 2.43 false positives per image.

## 5.2. Training Configuration

The inputs to the teacher network are  $224 \times 224 \times 3$  RGB patches, and the inputs to the student networks are either  $224 \times 224 \times 3$  RGB patches or  $224 \times 224 \times 10$  ACF patches. Patches are scaled by warping them to fit the input size, and RGB inputs are normalized using ImageNet mean and standard deviation. During training, patches are randomly flipped horizontally. The extraction of ACF features occur

Model	Direct Training	KD
ResNet-200	17.5%	—
ResNet-18	19.1%	<b>18.6%</b>
ResNet-18-Thin	<b>22.0%</b>	22.8%
ResNet-18-Small	<b>24.5%</b>	24.8%
AlexNet	23.3% [18]	—

Table 3: **Direct vs KD.** Comparison of log-average miss rate when trained directly from ground truth versus training with Knowledge Distillation,  $T = 2$ .

after the flip.

Training is performed through stochastic gradient descent with Nesterov Momentum 0.9 and weight decay 0.0005. We use a batch size of 16, an epoch size of 1000 iterations, a learning rate of 0.01 dropping by a factor of 5 every 20 epochs, and a total of 70 epochs. Since there are many more negatives patches than positive patches in our training set, we force a positive to negative ratio of 1 : 3 for each training batch. When combining soft and hard losses, hard losses are weighted with a value of  $\lambda = 0.5$ . For dropout during testing, we use a probability of 0.5. When estimating the covariance of teacher output, we compute the empirical covariance using 200 passes through the network. The models are trained with the Torch framework on a NVIDIA Titan X GPU with 12GB memory.

## 6. Experimental Evaluation

All of the evaluation results are reported on the Reasonable subset of the Caltech test set using the model at the epoch with the lowest log-average miss rate on the Reasonable subset of the Caltech validation set. For all of the student models tested, the best performing configuration was to use a single high-level (late) hint layer with teacher confidence and training directly with RGB inputs. A summary of all results can be found in Table 8 at the end of the paper. In the following sections, we analyze the impact of various design choices of the student network and methods for augmenting knowledge distillation.

### 6.1. Direct Training versus KD

We hypothesize that due to the low dimensional nature of the soft outputs of a binary classifier, KD would not provide additional information from which to learn a student network. Table 3 compares the various models trained directly from ground truth as well as the student models trained using standard Knowledge Distillation on the softmax logits. The temperature used for KD,  $T = 2$ , was picked heuristically after testing multiple values. As expected, we did not observe any significant changes in the miss rate between these two modes of training in our binary classification scenario. In fact, except for KD with ResNet-18, the re-

Model	Direct Training	KD+Hint
ResNet-200	17.5%	—
ResNet-18	19.1%	<b>18.1%</b>
ResNet-18-Thin	22.0%	<b>20.4%</b>
ResNet-18-Small	24.5%	<b>23.1%</b>

Table 4: Comparison of log-average miss rate when trained directly from the ground truth labels versus when matching hint layer outputs.

Model	Direct	Conf	Hint + Conf
ResNet-200	17.5%	—	—
ResNet-18	19.1%	18.2%	<b>18.0%</b>
ResNet-18-Thin	22.0%	20.7%	<b>20.3%</b>
ResNet-18-Small	24.5%	23.7%	<b>22.4%</b>

Table 5: Comparison of log-average miss rate when trained directly from the ground truth labels versus when trained with teacher output covariances, estimated either from the softmax logits or from the hint layer outputs.

maining student models perform worse when trained with standard KD.

## 6.2. KD from a High-level Hint Layer

We now evaluate our strategy of using a single fully connect (FC) layer, prior to the final binary FC layer as the hint layer. The intuition is that using a hint layer from the top of the teacher network will be more informative as it will encode high-level information about the correlation between high-level features. Furthermore, the inner hint layer is higher dimensional and can provide more information about what the student network should learn. As reported in Table 4, adding a hint layer improves training for all student models. This reinforces the idea that increasing the amount of information used for training models is beneficial.

## 6.3. Evaluation of Learning With Confidence

We have argued earlier that another pitfall of standard KD is the direct use of all teacher output without assessing the confidence of the teacher network. We now evaluate the impact that teacher confidence can have on the student training process. The covariance of the output over a single input image is computed using dropout described in Section 4.2.

Table 5 shows that estimating output covariances and training with our proposed loss function (Equation 6) improves the student models. There is slightly more improvement if the covariances are estimated from the hint layer outputs instead of the 2-dimensional softmax logits. Our experimental results show that the combination of hint layer learning and confidence weighted loss functions can im-

Model	RGB	ACF	ACF + Hint + Conf
ResNet-200	17.5%	19.6%	—
ResNet-18	19.1%	21.4%	<b>18.7%</b>
ResNet-18-Thin	22.0%	22.4%	<b>20.4%</b>
ResNet-18-Small	24.5%	25.2%	<b>23.4%</b>

Table 6: Comparison of log-average miss rate when trained directly from the ground truth labels with RGB inputs, ACF inputs, and when trained with ACF inputs with teacher output covariances estimated from hint layer outputs.

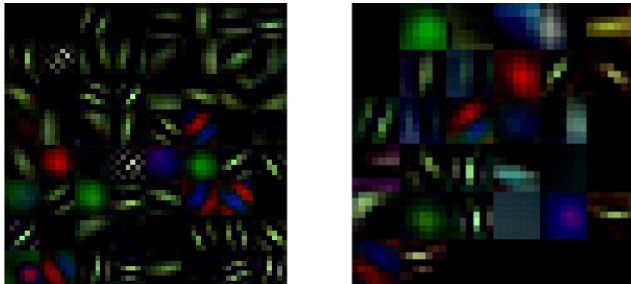


Figure 4: Visualization of the first convolutional layer from teacher network (left) and student network (right). The contrast has been adjusted for visibility.

	Student Correct	Student Fail
Teacher Correct	73.74%	21.12%
Teacher Fail	0.60%	4.54%

Table 7: Number of correct/fail matches between the student and teacher network.

prove performance in a meaningful way.

## 6.4. Impact of ACF Features on Student Learning

Our results in Table 6 are consistent with [18] in that a network trained directly using features like ACF as input is slightly under par compared to training with raw RGB inputs. This holds true even as the network size is significantly reduced, though the drop in performance for smaller models is not as severe. This is an interesting result which we believe is important to the research community despite the evidence contrary to our initial hypothesis, that smaller models would benefit from hand-designed features. The ability to back-propagate small corrections to the low-level feature extraction layers is indeed helpful, even for small networks.

Statistic		ResNet-200 (Teacher)		ResNet-18		ResNet-18-Thin		ResNet-18-Small	
		RGB	ACF	RGB	ACF	RGB	ACF	RGB	ACF
Log-Avg MR	Direct	<b>17.5%</b>	19.6%	19.1%	21.4%	22.0%	22.4%	24.5%	25.2%
	KD	—	—	18.6%	—	22.8%	23.1%	24.8%	—
	Conf	—	—	18.2%	—	20.7%	—	23.7%	—
	Hint	—	—	18.1%	—	20.4%	21.1%	23.1%	—
	Hint+Conf	—	—	<b>18.0%</b>	18.7%	<b>20.3%</b>	20.4%	<b>22.4%</b>	23.4%
#Parameters		63M (1×)		11M (6×)		2.8M (22×)		157K (400×)	
Speed		24ms (1×)		3ms (8×)		3ms (8×)		3ms (8×)	
Memory		5052MB (1×)		612MB (8×)		308MB (16×)		240MB (21×)	

Table 8: Summary of the results presented in this work. The configuration with the best log-average miss rate for each model is highlighted. Numbers in parenthesis indicate how much better the model is compared to the teacher.

Model	Time	Memory
ResNet-200	24ms	5377MB
ResNet-18	3ms	937MB
ResNet-18-Thin	3ms	633MB
ResNet-18-Small	3ms	565MB
Single Identity Layer	0.02ms	325MB

Table 9: Prediction time and memory usage for a size 16 batch of 224x224 patches.

## 7. Network Analysis

We compare ResNet-200 (teacher) with ResNet-18-Small-RGB-Hint-Conf (student) in terms of the agreement in predictions. We tabulate the correct and incorrect predictions for each model in Table 7. The teacher and student networks predict the same label 78.28% of the time. We show several example patches where there is both agreement and disagreement between the teacher and student model in Figure 2. The student did not predict any positive patches correctly that the teacher had predicted incorrectly. The patches where the student outperformed the teacher are indeed harder to classify, and could be a result of the student model being much smaller and thus more regularized. When we visualize the weights of the first convolutional layer in Figure 4 we can see that the student shares many of the same features as the teacher network. However, it is clear that the teacher network is able to represent a much more diverse set of low-level features. We can also see a redundancy in some of the features of the teacher network.

We also report the resource usage during test time on a NVIDIA Titan X in Table 9. It appears that modern GPUs are not affected very much by the number of channels in convolutional layers most likely due to high amounts of parallelization. While ResNet-18-Thin and ResNet-18-Small are much smaller in terms of the number of parameters, they are not significantly faster than ResNet-18. However, as ex-

pected, the memory usage is significantly decreased. Ignoring the fixed amount of memory used by the inputs and the system speed measured using a model with a single identity layer, ResNet-18-Small uses  $(5377 - 325)/(565 - 325) = 21\times$  less memory than ResNet-18.

## 8. Conclusion

We have shown that there is indeed a lot of redundancy in large deep neural networks. We have shown that it is possible to train a student network that contains 400 times fewer parameters while only observing a drop in log-average miss rate of 4.9%. The main gains of our approach utilizes the dimensionality of our hint layers. We also described a method of obtaining a measure of confidence from the teacher network, and demonstrated that taking this information into account during training can lead to considerable gains. Our student models perform 8x faster than the teacher with 21x less memory usage with only a drop of 2.8% in the log-average miss-rate.

## References

- [1] J. Ba and R. Caruana. Do deep nets really need to be deep? In *Advances in neural information processing systems*, pages 2654–2662, 2014. 3
- [2] R. Benenson, M. Omran, J. Hosang, , and B. Schiele. Ten years of pedestrian detection, what have we learned? In *ECCV, CVRSUAD workshop*, 2014. 6
- [3] Z. Cai, Q. Fan, R. Feris, and N. Vasconcelos. A unified multi-scale deep convolutional neural network for fast object detection. In *ECCV*, 2016. 1
- [4] W. Chen, J. T. Wilson, S. Tyree, K. Q. Weinberger, and Y. Chen. Compressing convolutional neural networks. *arXiv preprint arXiv:1506.04449*, 2015. 2
- [5] Y. Cheng, F. X. Yu, R. S. Feris, S. Kumar, A. N. Choudhary, and S. Chang. An exploration of parameter redundancy in deep networks with circulant projections. In *2015 IEEE International Conference on Computer Vision, ICCV 2015, Santiago, Chile, December 7-13, 2015*, pages 2857–2865, 2015. 2

- [6] N. Dalal and B. Triggs. Histograms of oriented gradients for human detection. In *Computer Vision and Pattern Recognition, 2005. CVPR 2005. IEEE Computer Society Conference on*, volume 1, pages 886–893. IEEE, 2005. 4
- [7] M. Denil, B. Shakibi, L. Dinh, M. A. Ranzato, and N. de Freitas. Predicting parameters in deep learning. In C. J. C. Burges, L. Bottou, M. Welling, Z. Ghahramani, and K. Q. Weinberger, editors, *Advances in Neural Information Processing Systems 26*, pages 2148–2156. Curran Associates, Inc., 2013. 1, 2
- [8] P. Dollár, R. Appel, S. Belongie, and P. Perona. Fast feature pyramids for object detection. *Pattern Analysis and Machine Intelligence, IEEE Transactions on*, 36(8):1532–1545, 2014. 2, 4, 5
- [9] P. Dollár, Z. Tu, P. Perona, and S. Belongie. Integral channel features. *Proc. British Machine Vision Conf*, 2009. 4
- [10] P. Dollár, C. Wojek, B. Schiele, and P. Perona. Pedestrian detection: An evaluation of the state of the art. *PAMI*, 34, 2012. 1, 5
- [11] Y. Gal and Z. Ghahramani. Dropout as a bayesian approximation: Representing model uncertainty in deep learning. *CoRR*, abs/1506.02142, 2015. 2, 4
- [12] S. Han, H. Mao, and W. J. Dally. A deep neural network compression pipeline: Pruning, quantization, huffman encoding. *arXiv preprint arXiv:1510.00149*, 2015. 2
- [13] S. J. Hanson and L. Y. Pratt. Comparing biases for minimal network construction with back-propagation. In *Advances in neural information processing systems*, pages 177–185, 1989. 2
- [14] B. Hassibi, D. G. Stork, and G. J. Wolff. Optimal brain surgeon and general network pruning. In *Neural Networks, 1993., IEEE International Conference on*, pages 293–299. IEEE, 1993. 2
- [15] K. He, X. Zhang, S. Ren, and J. Sun. Deep residual learning for image recognition. *arXiv preprint arXiv:1512.03385*, 2015. 1
- [16] K. He, X. Zhang, S. Ren, and J. Sun. Identity mappings in deep residual networks. *arXiv preprint arXiv:1603.05027*, 2016. 5, 6
- [17] G. Hinton, O. Vinyals, and J. Dean. Distilling the knowledge in a neural network. *arXiv preprint arXiv:1503.02531*, 2015. 2, 3
- [18] J. H. Hosang, M. Omran, R. Benenson, and B. Schiele. Taking a deeper look at pedestrians. *CoRR*, abs/1501.05790, 2015. 2, 5, 6, 7
- [19] Y. LeCun, J. S. Denker, and S. A. Solla. Optimal brain damage. In *Advances in Neural Information Processing Systems*, pages 598–605. Morgan Kaufmann, 1990. 1, 2
- [20] J. Li, X. Liang, S. Shen, T. Xu, and S. Yan. Scale-aware fast r-cnn for pedestrian detection. *arXiv preprint arXiv:1510.08160*, 2015. 1
- [21] B. Moons, B. De Brabandere, L. Van Gool, and M. Verhelst. Energy-efficient convnets through approximate computing. *arXiv preprint arXiv:1603.06777*, 2016. 2
- [22] A. Novikov, D. Podoprikin, A. Osokin, and D. P. Vetrov. Tensorizing neural networks. In C. Cortes, N. D. Lawrence, D. D. Lee, M. Sugiyama, and R. Garnett, editors, *Advances in Neural Information Processing Systems 28*, pages 442–450. Curran Associates, Inc., 2015. 3
- [23] I. V. Oseledets. Tensor-train decomposition. *SIAM J. Sci. Comput.*, 33(5):2295–2317, Sept. 2011. 3
- [24] S. Ren, K. He, R. Girshick, and J. Sun. Faster R-CNN: Towards real-time object detection with region proposal networks. In *Advances in Neural Information Processing Systems (NIPS)*, 2015. 1
- [25] A. Romero, N. Ballas, S. E. Kahou, A. Chassang, C. Gatta, and Y. Bengio. Fitnets: Hints for thin deep nets. *arXiv preprint arXiv:1412.6550*, 2014. 3
- [26] O. Russakovsky, J. Deng, H. Su, J. Krause, S. Satheesh, S. Ma, Z. Huang, A. Karpathy, A. Khosla, M. Bernstein, et al. Imagenet large scale visual recognition challenge. *International Journal of Computer Vision*, 115(3):211–252, 2015. 2
- [27] K. Simonyan and A. Zisserman. Very deep convolutional networks for large-scale image recognition. *arXiv preprint arXiv:1409.1556*, 2014. 1
- [28] S. Srinivas and R. V. Babu. Data-free parameter pruning for deep neural networks. In *Proceedings of the British Machine Vision Conference 2015, BMVC 2015, Swansea, UK, September 7-10, 2015*, pages 31.1–31.12, 2015. 2
- [29] L. Zhang, L. Lin, X. Liang, and K. He. Is faster r-cnn doing well for pedestrian detection? *arXiv preprint arXiv:1607.07032*, 2016. 1
- [30] S. Zhang, R. Benenson, and B. Schiele. Filtered channel features for pedestrian detection. In *Computer Vision and Pattern Recognition (CVPR), 2015 IEEE Conference on*, pages 1751–1760. IEEE, 2015. 4